Extraction, Optimization, and Characterization of Neem Seed Oil via Box-Behnken Design Approach

Ketema Beyecha Hundie[1*], Desalegn Abdissa Akuma[2], Abreham Bekele Bayu[3]

[1] School of Chemical engineering, Process Engineering, Jimma institute of Technology, Jimma University, Jimma, Oromia, Ethiopia
[2, 3] School of Chemical Engineering, Environmental Engineering, Jimma institute of Technology, Jimma University, Jimma, Oromia, Ethiopia

Abstract: This study was aimed at extracting, optimizing, and characterizing the neem seed oil through Box-Behnken design. The effects of extraction parameters such as temperature (50-80°C), particle size (0.15–0.3 mm), and time (60-180 min) were considered. The extraction of oil was studied using the soxhlet extraction process, applying n-hexane as a solvent. The quadratic model was suggested to demonstrate optimal extraction parameters of 132.677 min, 64.416˚C of temperature, and 0.212 mm of particle size using numerical optimization. The experimental yield of oil at optimum conditions 44.141%, which was close to the model-anticipated value. The physicochemical properties suggested that neem oil had an ash content of 2.1%, moisture content 4.61%, density 0.875 g/cm^3, viscosity 33.5 mm^2/s, specific gravity 0.88, saponification value 206.7 mg KOH/, iodine value 122.5 g I_2/100 g, acid value 1.81 mg KOH/g, and cetane number of 75. The extraction parameters had a significant effect on the yield of neem seed oil. However, the temperature and particle size had a higher effect compared to the extraction time. The most important unsaturated fatty acid is oleic acid (60.924 %). The properties of the oil revealed that the neem seed oil can be used as a potential source of material for industrial applications. It can be concluded that neem seeds have the potential to be used as industrial feedstocks in the future.

Keywords: Extraction, Neem Seed Oil, Property, Optimization

Submitted: December 22, 2021. **Accepted:** March 02, 2022.

Cite this: Beyecha Hundie K, Abdissa D, Bekele Bayu A. Extraction, Optimization, and Characterization of Neem Seed Oil via Box-Behnken Design Approach. JOTCSA. 2022;9(2):513–26.

DOI: https://doi.org/10.18596/jotcsa.1039997.

***Corresponding author. E-mail:** ketema.hundie@ju.edu.et.

INTRODUCTION

Since ancient times, humans have been searching in nature for resources that permit them to improve living conditions (1) and, consequently, sustain life span (2). Plant products or natural products show an important role in energy production(3), disease prevention and treatment through the enhancement of antioxidant activity (4), inhibition of bacterial growth, and modulation of genetic pathways (5).

One of these plants is *Azadirachta indica*, commonly known as the neem tree, which has been used since ancient times due to its potential applications and is currently emerging as a possible therapeutic agent for various diseases (6) and for industrial applications (7). The neem plant is mainly cultivated in several parts of the world such as Asia, Africa (8), America, and Europe (9), where it has been utilized through centuries, in medical folklore. It should be noted that different parts of the neem tree, including the bark, seeds, flowers, leaves, and oil, are related to the aforementioned medical folklore in the discussion of certain medical considerations such as hypertension, cancer, diabetes and heart diseases (10).

Approximations of alternative medicine utilized today as main care are in the order of about 80% for developing countries (11). In Ethiopia, most people use the neem trees without knowing its applications (12). In some regions, the rural people use neem leaves for village medicine, especially to cure malaria and diabetes (13). The use of neem seed oils as antimicrobial and food preservative agents is of concern because of several reported side effects of synthetic oils (14). Various investigators have presented that neem is a potential source of materials for drug delivery (10), cosmetic industry, pharmaceutical industry, and production of renewable energy that does not compete with the food-based feedstock (15).

Given the several uses of neem oil and its cooperativeness of transformation for different usages as stated earlier, it is crucial to explore the mechanism of extraction of the neem oil, which significantly minimizes extraction parameters, while maximizing the quantity an quality of the oil (16). The choice of mechanism and solvent will depend on the nature of the chemical compound to be extracted (17,18). The solvent extraction process is generally preferred for the extraction of the neem seed oil due to its low operating cost, higher oil yield, and lower turbidity compared to other methods (19). The solvent mostly employed for the extraction of oil is n-hexane due to its higher boiling point, stability, low corrosiveness, non-polarity, and high oil yield (20). Therefore, the goal of this work was the extraction, optimization, and characterization of neem seed oil utilizing the Box-Behnken experimental design.

EXPERIMENTAL DESIGN

Materials and chemicals

The neem seeds were collected from Jimma, Gibe, and Gambella, Ethiopia. The collected seeds were repeatedly washed and subsequently dried in an oven at 50°C for 24 hours to attain constant moisture content, and size reduction was conducted using laboratory mill.

All analytical grade chemicals were purchased from the chemical product suppliers (Piasa, Addis Ababa, Ethiopia).

The general Neem seed oil extraction process flow chart is indicated in Figure 1.

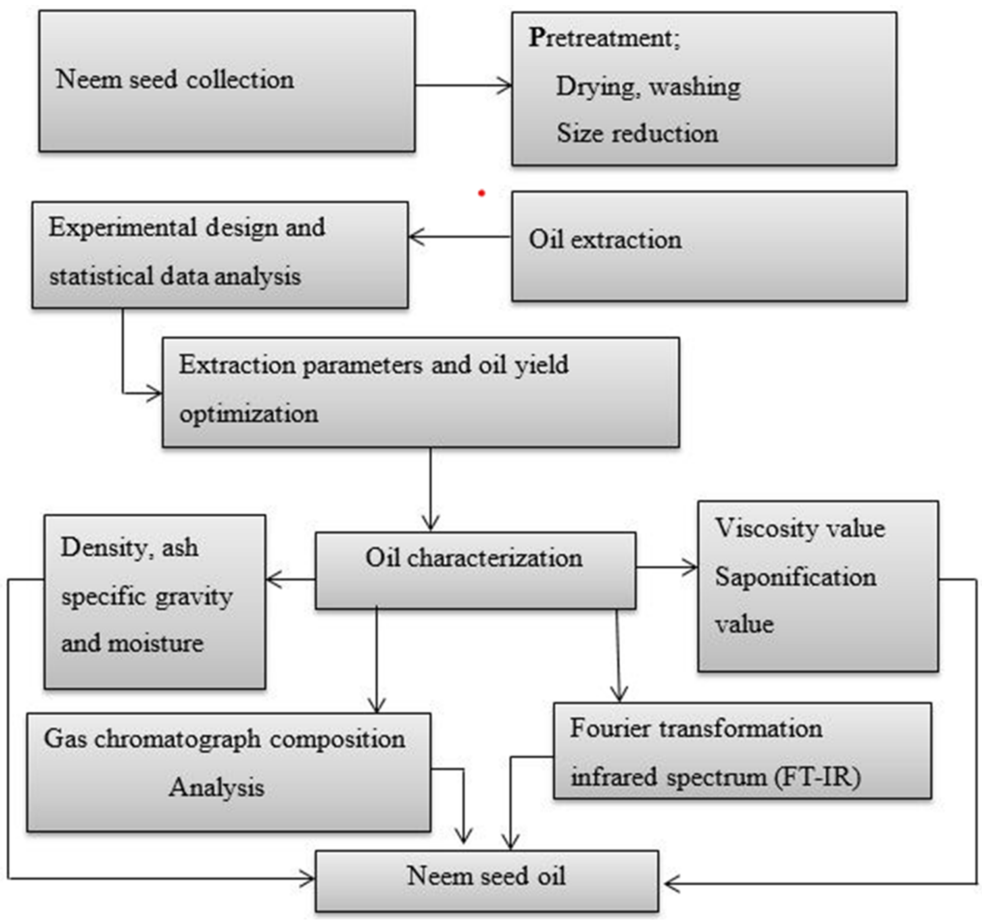

Figure 1: Neem seed oil extraction process flow chart.

Methodology

Oil Extraction

The extraction of neem seed oil was conducted as shown in Figure 1. A 500 ml soxhlet apparatus was utilized with the organic solvent n-hexane. The measured powder of the sample was added to a thimble and placed in a condenser. A flask containig a measured volume of the solvent was placed at the end of the soxhlet apparatus, and a condenser was fixed at the bottom. The parameters were adjusted to a temperature of 50-80˚C, a particle size of 0.15-2 mm and a time of 60-180 min. At the time interval, the oil was collected in the volumetric flask, then centrifuged to separate the solid part from the solution, and evaporated, using a rotary evaporator to get solvent-free oil. The procedure was done in accordance with the standard previously reported (21), for the evaluation of the oils. The yield of oil was determined using Eq. (1).

$$\text{Oil Yield}=(\%)=\frac{W_1-W_2}{W_1*100}$$

(Eq. 1)

Where: W_1=Sample weight initially placed in the thimble and W_2= sample weight after dried in the oven.

Experimental design and statistical data analysis

The experimental design to analyze the process parameters was carried out utilizing the Box-Behnken design method with the aim of parameter optimization for oil extraction. The Box-Behnken design consisted of three variables: time (60-180 min), temperature (50-80˚C) and particle size (0.15-0.3 mm) as shown in Table 1. A total of 15 experimental runs (Table 2) were done with replication.

Table 1: Box-Behnken design parameters for neem seed oil extraction.

Factors	Codes	Minimum	Medium	Maximum
Reaction time (min)	A	60 (-1)	120(0)	180 (+1)
Particle size (mm)	B	0.15 (-1)	0.225(0)	0.3 (+)
Reaction temperature (^{0}C)	C	50 (-1)	65(0)	80 (+1)

Statistical Data Analysis

The results obtained from the experiment data were evaluated employing the Box-Behnken design model. The model equation was examined using multiple regression analysis to measure the response through the linear interaction and quadratic effects of the process parameters suggested by the model.

$$Y=b_0+\sum_{i=1}^{n} b_i X_i+\sum_{i=1}^{n} b_{ij} X_i^2+\sum_{i=1}^{n} b_{ii} X_{ii,} X_{ij} \quad \text{(Eq. 2)}$$

Where: Y is predicted yield %, i and j indicate linear and quadratic coefficients respectively, b_o is the intercept, b_i is the linear model coefficient, n is the number of variables and X_{ii}, and X_{ij} are self-interaction and interaction between variables respectively.

Property of the Neem Seed Oil

Physicochemical property

The properties of neem seed oil such as specific gravity, density, iodine value, saponification value, and acid value, were analyzed according to the Association of Official Analytical Chemists (AOAC (1990) (22) and American Society of Testing Material (ASTM) (23,24).

Gas Chromatography of the Fatty Acid Composition Analysis

Gas chromatography-mass spectrometry was employed to analyze the fatty acid composition. It was carried out by electron ionization fashion on a GC-MS (GC = Agilent 8856B and MS =Agilent 6742 manufactured at German) system with a blended capillary column of 4.5% phenols-methyl Silphium (20 m × 0.30 mm × 0.30 mm; PN =18211-S-342HP-6 M-S) coupled to the mass detector for the sample analysis.

Fourier Transform Infrared Spectroscopy (FT-IR) Functional Group Analysis

The infrared spectra of the oil were recorded with a NaBr (alkalic halogenide)-pellet method utilizing a Tensor 30 FTIR spectrometer (Brukerash Optik, Gnch, USA) at a frequency ranging between 4000–400 cm^{-1} and a wavenumber precision of 0.1 cm^{-1}. All spectra were post-processed using an OBUS software (Brukerash Optik).

RESULTS AND DISCUSSION

Experimental Design and Statistical Data Analysis

The results of the Box-Behnken experimental design, shown in Table 2, indicated that oil yields were between 16.4 and 43.9% corresponding to extraction parameters of temperature (65˚C), particle size (0.225 mm), and extraction time (120 min).

The experimental values were in agreement with the predicted ones obtained from Eq. (2) and generated in Eq. (3), as shown in Figure 2. An acceptable correspondence between the actual and predicted values of the yield was observed. The good correspondence between the predicted value, R-squared value (99.85%), R-predicted squared value (97.69%), and R-adjusted squared value (99.58%)

indicated a linear correspondence between the predicted and experimental values (Table 4). The results affirmed that both R-adjusted squared and R-squared values were close to unity, which suggested that the model gave a good approximation of response in the considered range.

Table 2: Experimental design parameters Vs oil yields (actual and predicted values).

Run order	Factors			Responses (yield %)		Residual error
	A: Temperature	B: Particle size	C: Time	Actual	Predicted	
unit	^{0}C	mm	min	%	%	
1	65	0.15	180	38.1	38.11	-0.0075
2	65	0.15	60	42.02	42.64	-0.6225
3	80	0.225	180	20.82	21.13	-0.3100
4	65	0.225	120	43.9	43.73	0.1667
5	50	0.225	60	36	35.69	0.3100
6	65	0.3	60	32.1	32.09	0.0075
7	65	0.3	180	29.49	28.87	0.6225
8	65	0.225	120	43.5	43.73	-0.2333
9	80	0.225	60	25.12	24.82	0.3050
10	50	0.3	120	26.01	26.33	-0.3175
11	65	0.225	120	43.8	43.73	0.0667
12	50	0.225	180	31.31	31.62	-0.3050
13	80	0.3	120	16.4	16.71	-0.3125
14	80	0.15	120	25.86	25.54	0.3175
15	50	0.15	120	37.6	37.29	0.3125

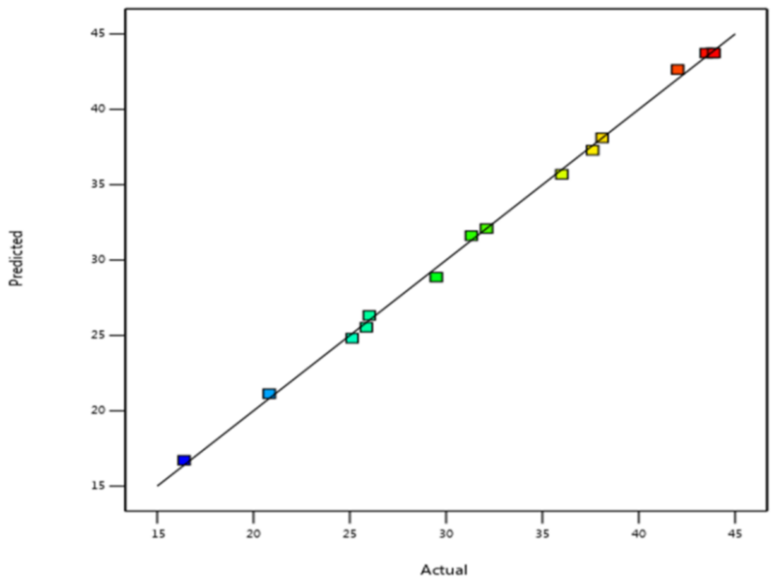

Figure 2: Experimental yield Vs predicted yield of the oil in percentage.

The accuracy of the formulated model has been verified by analyzing the residuals plot. The difference between the actual and calculated response is known as the residuals. Hence, for each experimental data set, there is a residual (25). The normal statistical distribution of the residuals is a prove of observational errors randomization. Studentized residuals are determined by separating the normalized residuals with their standard difference prediction, where they are fitted with a normal statistical distribution function (26). The residual-standard plots in Figure 3 were all in ±6.25 intervals, suggesting that the model was consistent with the experimental value with no error registered (25).

The experimental run versus the residuals was plotted as shown in Figure 3 (b), which outlines the residual result for each run. The plot indicates the degree of deviation between the test and anticipated values. The fitted regression analysis was very close to the plot, as the studentized residuals were placed within the ±6.25 range. The precision of the quadratic demonstration was affirmed by the random distribution of residuals, as indicated in Figure 3(b). Therefore, it can be concluded that a satisfactory description of the oil extraction process was accomplished by the regression model and it does not spoil the constant variance assumption (27).

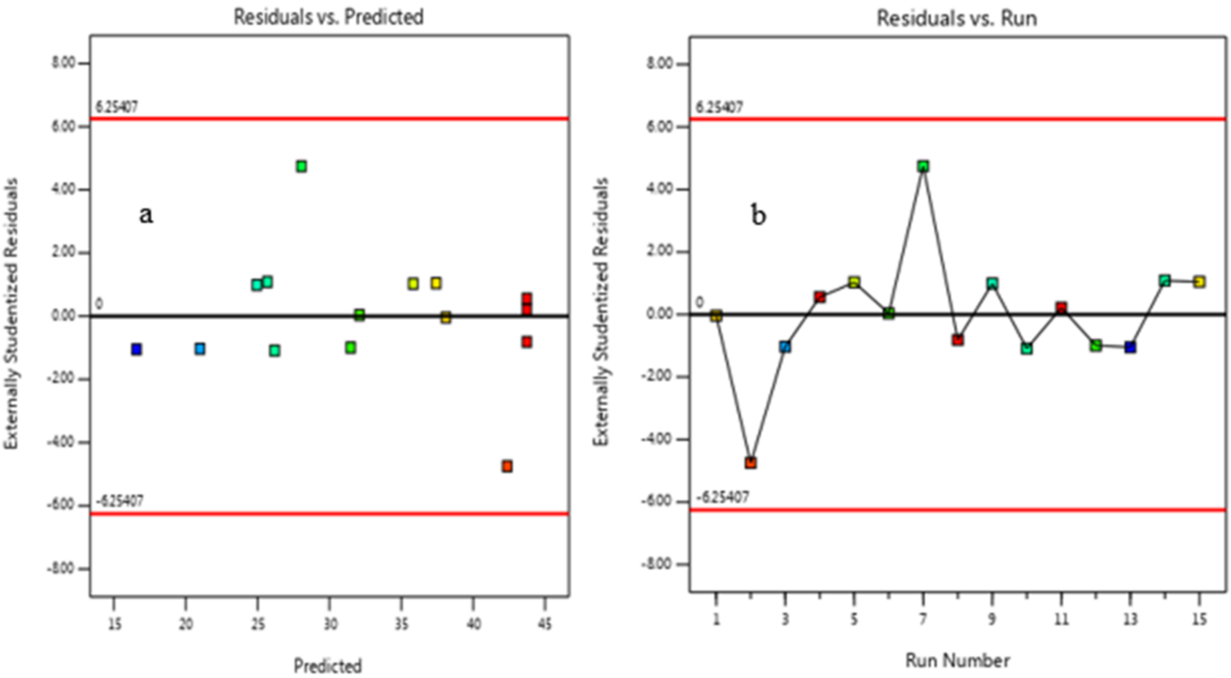

Figure 3: Residual Vs prediction (a) and Residual Vs Number of the runs (b).

The analysis of ANOVA is shown in Table 3. The model F-value of 367.49 and P-values of less than 0.0500 indicated that model terms were significant. In this case, all linear terms (temperature: A, particle size: B and time: C) and quadratic terms (A^2, B^2, and C^2) were significant models. However, A-squared (A^2) term had the highest coefficient, which showed that curvature along this dimension was very significant. The ANOVA indicated in Table 3, and Eq(3) showed the largest degree of significance for this term and the model as a whole.

Table 3: ANOVA analysis for Quadratic model.

Source	Sum of Squares	df	Mean Square	F-value	p-value	
Model	1082.84	9	120.32	367.49	< 0.0001	Significant
A-Temperature	228.12	1	228.12	696.79	< 0.0001	
B-Particle size	195.82	1	195.82	598.12	< 0.0001	
C-Time	30.11	1	30.11	91.97	0.0002	
AB	1.13	1	1.13	3.46	0.1218	
AC	0.0380	1	0.0380	0.1161	0.7471	
BC	0.4290	1	0.4290	1.31	0.3041	
A^2	548.70	1	548.70	1675.97	< 0.0001	
B^2	95.11	1	95.11	290.52	< 0.0001	
C^2	38.53	1	38.53	117.69	0.0001	
Residual	1.64	5	0.3274			
Lack of Fit	1.55	3	0.5168	11.93	0.0784	Not significant
Pure Error	0.0867	2	0.0433			
Cor Total	1084.48	14				

The lack of fit test is also shown for the regression model analysis. It indicated the model's power to depict the relationship between the input and output parameters sufficiently. The model could indicate a lack of fit due to the comportment of unusually greater residuals existing from fitting the model or omitting from the model various necessary terms (28). The lack of fit value for the extraction of the oil model indicates an F-value of 11.93 and a P-value of 0.0784 in this study. This outcome has shown that the quadratic model was well fitted to the experimental data. When the F-ratio gets so high, that the p-value falls below 0.05, then with

95% confidence, one or more of the factors was affecting the measured response (29).

The coefficient of prediction represents the expected change in response per unit change in factor value when all remaining factors are held constant (Table 4). The intercept in an orthogonal design is the overall average response of all the runs. The coefficients are adjustments around that average based on the factor settings. When the factors are orthogonal, the VIFs are 1; VIFs greater than 1 indicate multi-collinearity. the higher the VIF, the more severe the correlation of factors. As a rough rule, VIFs of less than 10 are tolerable (30).

Table 4: Coefficients in terms of coded factors and coefficient of determination.

Coefficients in Terms of Coded Factors						
Factor	Coefficient Estimate	df	Standard Error	95%CI Low	95%CI High	VIF
Intercept	43.73	1	0.3303	42.88	44.58	
A-Temperature	-5.34	1	0.2023	-5.86	-4.82	1.00
B-Particle size	-4.95	1	0.2023	-5.47	-4.43	1.00
C-Time	-1.94	1	0.2023	-2.46	-1.42	1.00
AB	0.5325	1	0.2861	-0.2029	1.27	1.00
AC	0.0975	1	0.2861	-0.6379	0.8329	1.00
BC	0.3275	1	0.2861	-0.4079	1.06	1.00
A^2	-12.19	1	0.2978	-12.96	-11.42	1.01
B^2	-5.08	1	0.2978	-5.84	-4.31	1.01
C^2	-3.23	1	0.2978	-4.00	-2.46	1.01
Fit Statistics						
Coefficients				**Value**		
R-squared R^2				0.9985		
Adjusted R^2				0.9958		
Predicted R^2				0.9769		
Adeq Precision				57.8375		
Std. Dev.				0.5722		
Mean				32.80		
C.V. %				1.74		

C.V = coefficient of variation, Std.Dev. = standard deviation, VIF=Variance inflation factor

The quadratic models of regression analysis, suggested by the model, were expressed as follows in terms of coded factors:

$$\text{Yield (\%)} = 43.73-5.34\,A-4.95\,B-1.94\,C+0.5325\,A\,B+0.0975\,A\,C+0.3275\,BC$$
$$-12.\,A^2-5.08\,B^2-3.23\,C^2 \quad \text{(Eq. 3)}$$

The equation in terms of coded parameters can be used to form predictions about the response to given levels of each parameter. By default, the high levels of the parameters are coded as low levels (-1) and high levels (+1). The coded equations help to describe the relative influence of the variables by comparing the coefficients of the variables (31).

Effect of Extraction Parameters on the Yield of Oil

Effect of extraction temperature

The extraction process can occur at various temperatures based on the used solvent. Temperature is a critical parameter as it determines the reaction rate and yield of the produced oil (32). To find out the significance of extraction temperature on the conversion of oil, experiments were carried out at 50-80 ˚C (Figure 4(a)). The effect of temperature on a reaction can be described through the theory of reaction kinetics. Enhancing the temperature will result in an enhancement fraction of particles that have greater speed and therefore have a higher kinetic rate, which results from the maximum yield of extraction (32). The highest yield of the oil was 43.9 % at an extraction temperature of 65°C. The yield of the oil was decreased beyond 65°C of extraction temperature; higher temperature accelerates the formation of saponification reaction which results in soap formation, as well as further increment of temperature is described to have an adverse effect on the conversion of the yield (31). In addition, maximum temperature resulted in a decrement of the yield, as hexane is lost because it starts to evaporate as the temperature approaches its boiling point (33).

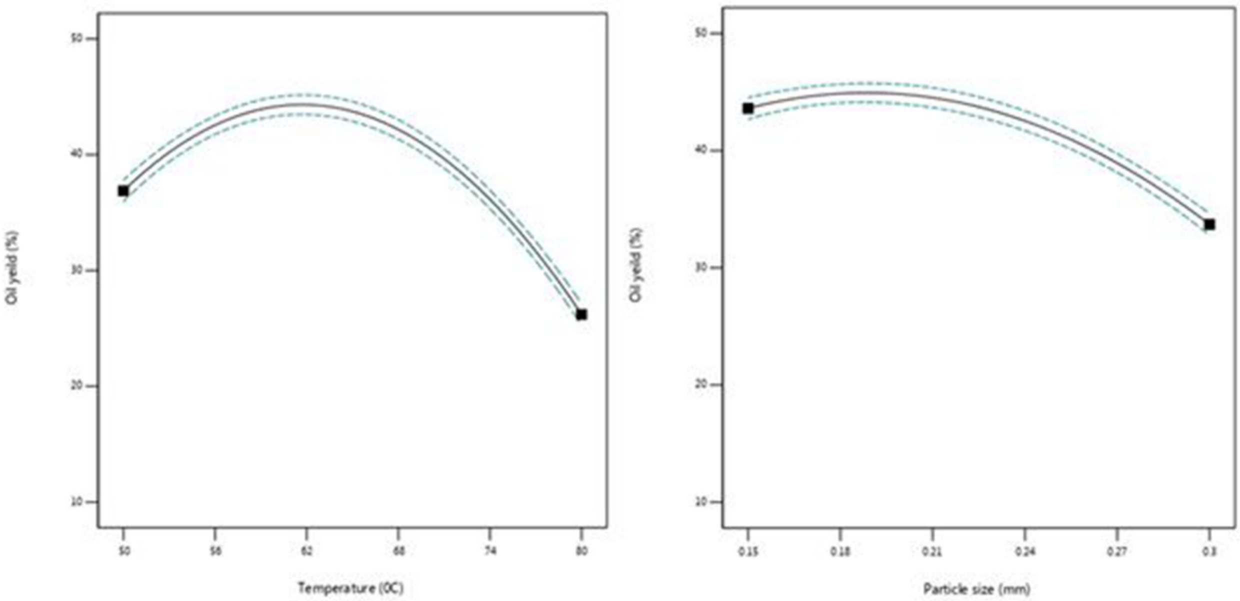

Figure 4: Effect of temperature (a) and particle size (b) on the extraction yield of oil.

Effects of particle size

It was indicated that the effectiveness of the biomass process is expected to be dependent on particle size (34). At optimum particle size, it is expected to bring up the speed of reaction between components; since the rate of reaction is influenced by the raw material accessibility and medium size of the molecule for better yield, while the bigger size of the molecule indicates a small amount of oil yield (35,36). Figure 4(b) shows the effects of particle size on oil yield while al other parameters are kept constant at zero levels; increasing the particle size to the maximum while keeping the other parameters constant results in a low oil yield. Increasing the particle size from 0.15-0.225 mm, results in the maximum yield of oil. The particle size of 0.225 mm was found to be the optimum point at which the maximum yield of oil was achieved. A particle size of above 0.3 mm has been observed to give an optimum yield of oil in the extraction of solid coconut oil (37–39).

Effect of extraction time

Another important process parameter that affects the yield of oil extraction is time. The extraction time was studied between 60-80 min. The effect of extraction time on the yield of neem seed oil was shown in Figure 5. It could be determined that the yield of oil increased as extraction time moved up from 60 to 120 min and peaked at 120 min. This observation proposes that at the initial time of extraction, more oil was expelled from the neem seed (40,41). However, the rate was diminished with the increasing duration of time. At a longer extraction time, the negative impact of this factor on the yield was also considered (42,43).

Perturbation plot

The perturbation plot indicates the comparability between all parameters at a preferred point in the studied design space. The perturbation diagram for the yield of the extracted neem seed oil is demonstrated in Figure 6. The yield of extraction was described by changing only one variable over its range while the other variables were held constant. The plot shows the effect of all parameters at a central point in the design space (such as extraction time, particle size, and extraction temperature).

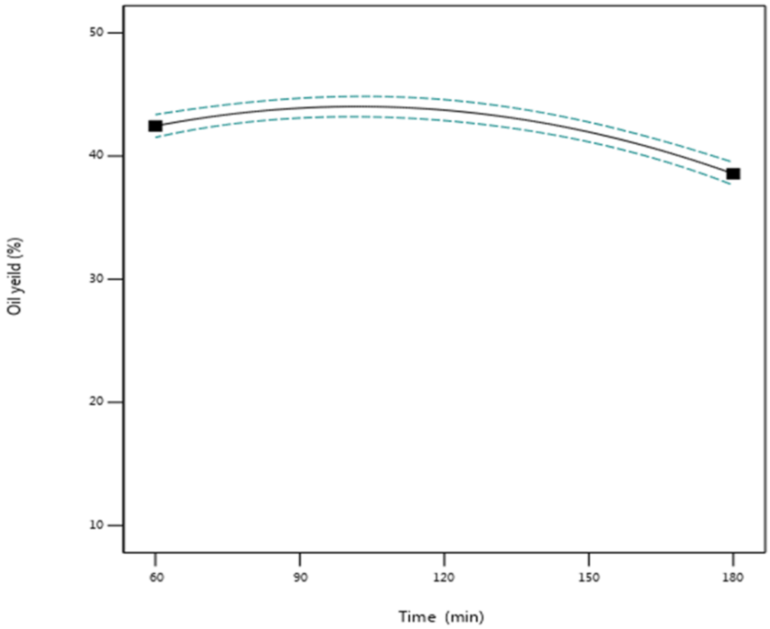

Figure 5: Effect of extraction time on the extraction yield of sandalwood oil.

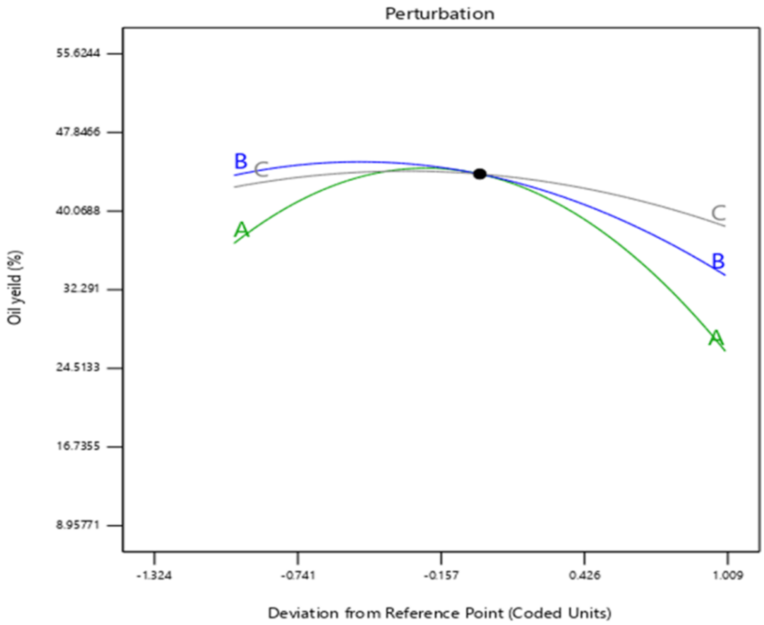

Figure 6: Perturbation plot for the extraction yield of neem oil response (A: Temperature, B: Particle size and C: Time).

All variables pointed to a negative result on the yield of extraction. The comparatively flat line of extraction time (C) shows a lower effect of this variable on the extraction yield of neem seed oil in the design space. It can be shown from Eq. (3) and Table 3 that extraction temperature and particle size had significant curvature effects on the yield. Through this comparability of coefficients in Eqn. (3), the majority of the significant variables were identified. In this way, the order of positive effects of the interaction terms on the yield of extraction was A-B, A-C and B-C; while the remaining individual and quadratic terms had a negative influence on the yield of oil.

Optimization of oil extraction parameters

The goal of the study was to identify the optimal parameters for oil extraction. The optimized parameters were derived from the quadratic regression analysis proposed by the Box-Behnken design. Using Box-Behnken design, the optimal values for the developed regression model (Eqn. 2) and according to the described optimization criteria for selected variables, the optimization was conducted using the numerical method. The model was applied by setting independent variables in the range with the goal of oil yield maximization. The model anticipated an optimal yield of oil, 44.081% at 64.416˚C extraction temperature, 0.212 mm particle size, and 132.677 min of extraction time with the maximum desirability of 1 among 100 solutions proposed. This means it is possible to select a series of combinations of the optimum parameters, which will enable maximum yield of oil. In addition, Figure 7 indicates the optimized process parameters for the extraction yield of neem seed oil. The experimental yield of oil (44.141%) at optimal parameters is close to the model-anticipated value of 44.081% within 0.136% of error value.

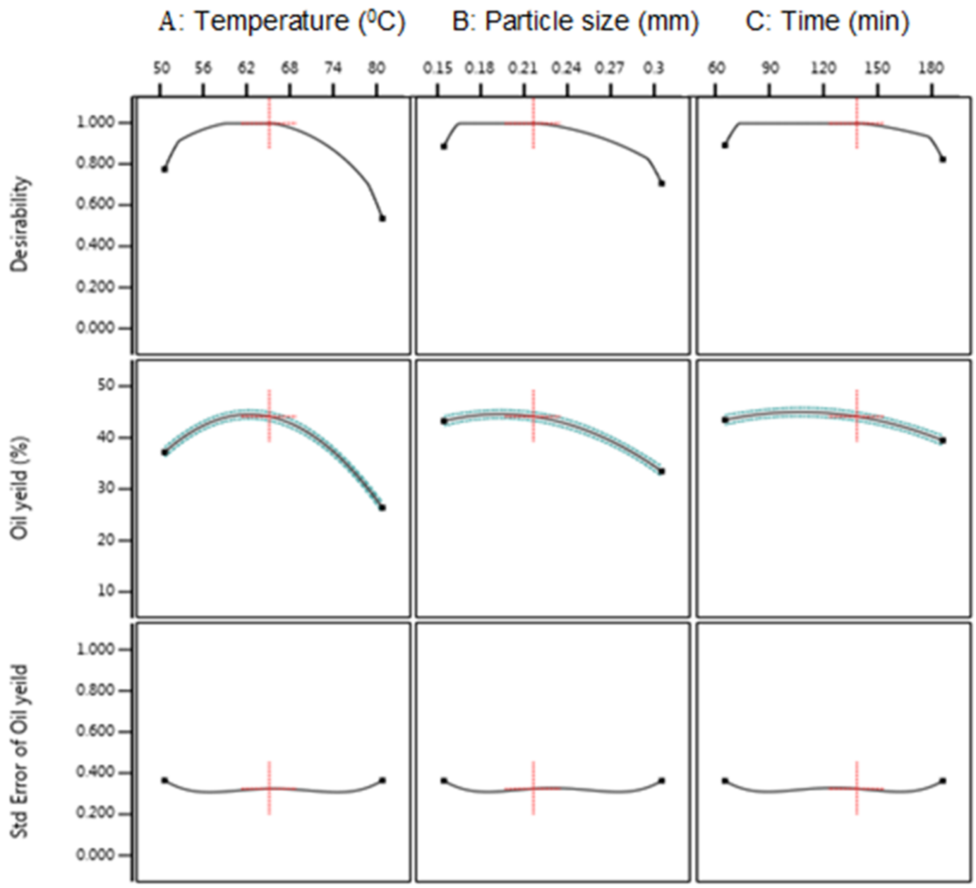

Figure 7: Shows the output (independent and dependent variables) of numerical optimization of the developed mathematical models.

Analysis of Properties of Neem Seed Oil

Physicochemical property

Different properties of the oil were analyzed according to AOAC (1990) and ASTM standards with modification as shown in Table 5.

The specific gravity of all the oils ranged from 0.84 to 0.91, which corresponds to the standard limit of 0.87-0.90 for non-edible oils (26). Density and gravity are important parameters for oil used in diesel fuel injection systems. The values must be maintained within tolerable limits to allow optimal air to fuel ratios for complete combustion. High-density biodiesel or its blend can lead to incomplete combustion and particulate matter emissions (37–39). In this study, 0.875 g/cm^3 of density and 0.86 of specific gravity were obtained. Therefore, if this oil is used for biodiesel production, it will be safe since it fulfils the required criteria.

The ash content in oils is an important variable, at considerable quantity, to indicate the quality of the oil. An ash content of 2.1% has been recorded. Small ash content indicated that the extracted neem oil can be ignitable with a low amount of ash and can be used for biofuel production (44).

Iodine value is an indication of the unsaturation of fats and oils. The greater iodine value shows the higher unsaturation of oils and fats (26). Oils with iodine values greater than 120 are grouped as drying oils; those with iodine values of 60–120 are grouped as semi-drying oils; and those with iodine values below 60 are regarded as non-drying oils. In this study, the iodine value of the neem oil was 122.5 mgI$_2$/g, which is close to the standard specified by ASTM D763 (120 mg I$_2$/g) for dry oil, and this oil can be used in the cosmetic industry. People choose dry oils since they absorb into the skin within seconds of application, meaning that dry oils indicate the same moisturizing advantages as wet oils, without missing a sticky residue on the hair or skin (45).

Acid values identify the appearance of oxidation products and corrosive free fatty acids as well as the degree of the lubricant's abasement. This is a necessary factor used to determine the quality of oil, since the lower the free fatty acid, the better the quality of the oil. More acidic value can contribute to severe corrosion in the internal combustion engine and fuel supply system (46). In this study 1.81(mg KOH/g) of acid value was recorded.

The saponification value is utilized in checking out debasement. The higher saponification value shows the existence of a higher percentage of fatty acids in the oil (44) and hence involves the possible trend to make soap; those difficulties in separation of products if used for producing biodiesel. This would also suggest that utilizing the oils for the production of biodiesel would result in a very low yield of the methyl ester. In this study, 206.7mg KOH/g of saponification value of oil was obtained, which is within the limit of ASTM standard.

Table 5: Physiochemical properties of neem seed oil.

Components	**Value**	**ASTM** 763 **standard**
Density (g/cm^3)	0.875	0.8-0.9
Moisture contents (%)	4.61	0.3-6.0
Ash contents (%)	2.31	1.5-4.5
viscosity (mm^2/s)	33.5	25-35.5
Iodine value (mg I_2/100g)	122.5	120
Saponification Value (mg KOH/g)	206.7	200-220
Acid value (mg KOH/g)	1.81	1.5-2.4

Fatty acid composition analysis with gas chromatography

The fatty acid constitution of the extracted neem seed oil was studied via the gas chromatography-mass spectrometry method. Five types of fatty acids were detected. As shown in Table 5, the predominant fatty acid was oleic acid adopted by palmitic acid, caprylic acid, stearic and myristic acid, respectively. The chromatographic-mass spectrometry study revealed a considerable amount of unsaturated fatty acids in the oil of neem seeds. The fatty acid constitution of oil and its structures are presented in Table 6.

Table 6: Fat acid composition of neem seed oil.

Fatty acid type	Formula	Composition (%)
saturated fat acid		
Caprylic acid	$C_8H_{16}O_2$	16.621
Myristic acid	$C_{14}H_{28}O_2$	0.0058
Palmitic acid	$C_{16}H_{32}O_2$	22.443
Stearic acid	$C_{18}H_{36}O_2$	0.0062
Total		39.076
Unsaturated fatty acid		
Oleic acid	$C_{18}H_{34}O_2$	60.924
Total		60.924

Fourier Transform Infrared Spectroscopy (FT-IR) Functional Group Analysis

The results of the FT-IR analysis of the neem seed oil is shown in Figure 8. The assimilation peak at different wavelengths was also indicated. The peak at 3006.26 cm^{-1} is due to C-H asymmetrical stretch and the absorption peak at 2923.78 cm^{-1} and 2855.25 are due to the C-H symmetric and antisymmetric stretch of the methyl group from the lipids (44). Peaks present at 1460.55 cm^{-1} and 1376.06 cm^{-1} are attributed to the C-H antisymmetric and symmetric deformation vibrations, respectively (46). The band at peaks of 1095.86 cm^{-1}, 1236.83 cm^{-1}, 1160.38 and 1236.83 cm^{-1} corresponds to the C-O stretching vibration (46). The absorption at 1743.66 cm^{-1} is also due to the C-O stretch and the peak at 720.79 cm^{-1} is due to the C-H bond from the long branch of alkane (40,41).

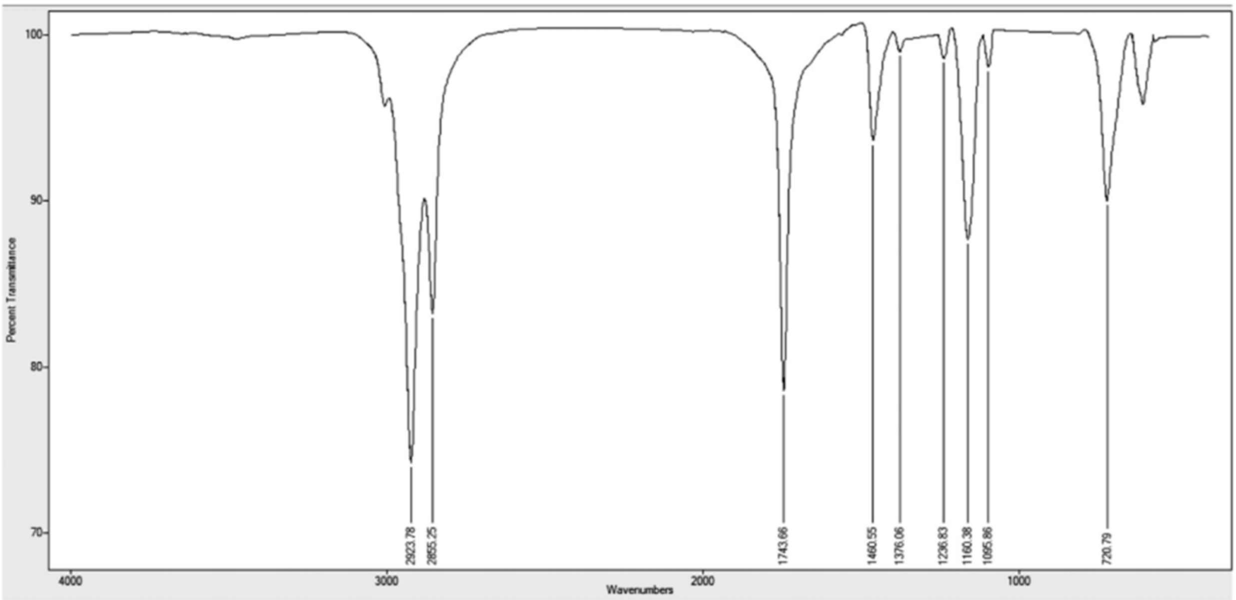

Figure 8: FTIR spectral analysis of neem seed oil at a frequency of 4000–400 cm^{-1}.

CONCLUSION

Neem seed oil was extracted using the Soxhlet extraction method. The effect of different extraction variables, such as extraction temperature, particle size, and extraction time, on oil yield was investigated by using Box-Behnken experimental design. The quadratic model was suggested to demonstrate optimum extraction parameters. Applying the numerical optimization of the desirability maximization technique, 132.677 min of extraction time, 64.416˚C of extraction temperature, 0.212 mm of particle size, and 44.081% of oil yield were obtained at selected desirability. The experimental yield of oil (44.141%) at optimal parameters is close to the model-anticipated value of 44.081% within 0.135% of the error value. The study shows that the effects of temperature and particle size are found to be more significant compared to extraction time. The physicochemical characteristics of the extracted oil were also determined by using standard methods. The physicochemical properties of the oil reveal that the neem seed oil can be considered as a potential source of material for different products. The most common fatty acids in the neem seeds were oleic acid (60.924%), palmitic acid (22.443%), and caprylic acid (16.621%). The obtained results indicate the prospect of using neem seeds as a potential raw material in the industrial field in the future.

CONFLICT OF INTEREST

The author wishes to confirm that there is no conflict of interest associated with this paper for any material as well as financial.

ETHICAL APPROVAL

This article does not contain any studies with human participants or animals performed by any of the authors.

ACKNOWLEDGMENTS

Thanks to the School of Chemical Engineering as well as Addis Ababa University Institute of Technology and Colleagues of natural science for their support for this work.

FUNDING

The authors are grateful to Jimma University Institute of Technology for financial support for MEGA GRANT, RPD/JiT/0164/12/Code JiT_2019_36 research.

REFERENCES

1. Anand S, Sen A. Human Development and Economic Sustainability. World Development. 2000 Dec;28(12):2029–49. <DOI>.

2. Tomizawa A, Zhao L, Bassellier G, Ahlstrom D. Economic growth, innovation, institutions, and the Great Enrichment. Asia Pac J Manag. 2020 Mar;37(1):7–31. <DOI>.

3. Ram S, Mitra M, Shah F, Tirkey SR, Mishra S. Bacteria as an alternate biofactory for carotenoid production: A review of its applications, opportunities and challenges. Journal of Functional Foods. 2020 Apr;67:103867. <DOI>.

4. Ashaolu TJ. Immune boosting functional foods and their mechanisms: A critical evaluation of probiotics and prebiotics. Biomedicine & Pharmacotherapy. 2020 Oct;130:110625. <DOI>.

5. Rodrigo R, Miranda A, Vergara L. Modulation of endogenous antioxidant system by wine polyphenols in human disease. Clinica Chimica Acta. 2011 Feb;412(5–6):410–24. <DOI>.

6. Fernandes SR, Barreiros L, Oliveira RF, Cruz A, Prudêncio C, Oliveira AI, et al. Chemistry, bioactivities, extraction and analysis of azadirachtin: State-of-the-art. Fitoterapia. 2019 Apr;134:141–50. <DOI>.

7. Patel SM, Nagulapalli Venkata KC, Bhattacharyya P, Sethi G, Bishayee A. Potential of neem (Azadirachta indica L.) for prevention and treatment of oncologic diseases. Seminars in Cancer Biology. 2016 Oct;40–41:100–15. <DOI>.

8. Patra JK, Das G, Lee S, Kang S-S, Shin H-S. Selected commercial plants: A review of extraction and isolation of bioactive compounds and their pharmacological market value. Trends in Food Science & Technology. 2018 Dec;82:89–109. <DOI>.

9. Tschoeke PH, Oliveira EE, Dalcin MS, Silveira-Tschoeke MCAC, Sarmento RA, Santos GR. Botanical and synthetic pesticides alter the flower visitation rates of pollinator bees in Neotropical melon fields. Environmental Pollution. 2019 Aug;251:591–9. <DOI>.

10. Islas JF, Acosta E, G-Buentello Z, Delgado-Gallegos JL, Moreno-Treviño MG, Escalante B, et al. An overview of Neem (Azadirachta indica) and its potential impact on health. Journal of Functional Foods. 2020 Nov;74:104171. <DOI>.

11. Büyüközkan G, Mukul E, Kongar E. Health tourism strategy selection via SWOT analysis and integrated hesitant fuzzy linguistic AHP-MABAC approach. Socio-Economic Planning Sciences. 2021 Apr;74:100929. <DOI>.

12. Megersa M, Jima TT, Goro KK. The Use of Medicinal Plants for the Treatment of Toothache in Ethiopia. Evidence-Based Complementary and Alternative Medicine. 2019 Aug 20;2019:1–16. <DOI>.

13. Chowdhury MSH, Koike M. Therapeutic use of plants by local communities in and around Rema-Kalenga Wildlife Sanctuary: implications for protected area management in Bangladesh. Agroforest Syst. 2010 Oct;80(2):241–57. <DOI>.

14. Sharma S, Barkauskaite S, Jaiswal AK, Jaiswal S. Essential oils as additives in active food packaging. Food Chemistry. 2021 May;343:128403. <DOI>.

15. Mitra S, Ghose A, Gujre N, Senthilkumar S, Borah P, Paul A, et al. A review on environmental and socioeconomic perspectives of three promising biofuel plants Jatropha curcas, Pongamia pinnata and Mesua ferrea. Biomass and Bioenergy. 2021 Aug;151:106173. <DOI>.

16. Seljak T, Buffi M, Valera-Medina A, Chong CT, Chiaramonti D, Katrašnik T. Bioliquids and their use in power generation – A technology review. Renewable and Sustainable Energy Reviews. 2020 Sep;129:109930. <DOI>.

17. Sprakel LMJ, Schuur B. Solvent developments for liquid-liquid extraction of carboxylic acids in perspective. Separation and Purification Technology. 2019 Mar;211:935–57. <DOI>.

18. Belwal T, Ezzat SM, Rastrelli L, Bhatt ID, Daglia M, Baldi A, et al. A critical analysis of extraction techniques used for botanicals: Trends, priorities, industrial uses and optimization strategies. TrAC Trends in Analytical Chemistry. 2018 Mar;100:82–102. <DOI>.

19. Ghazanfari N, Mortazavi SA, Yazdi FT, Mohammadi M. Microwave-assisted hydrodistillation extraction of essential oil from coriander seeds and evaluation of their composition, antioxidant and antimicrobial activity. Heliyon. 2020 Sep;6(9):e04893. <DOI>.

20. Tomić M, Ljubojević M, Mićić R, Simikić M, Dulić J, Narandžić T, et al. Oil from Koelreuteria paniculata Laxm. 1772 as possible feedstock for biodiesel production. Fuel. 2020 Oct;277:118162. <DOI>.

21. Hasni K, Ilham Z, Dharma S, Varman M. Optimization of biodiesel production from Brucea javanica seeds oil as novel non-edible feedstock using response surface methodology. Energy Conversion and Management. 2017 Oct;149:392–400. <DOI>.

22. Falowo OA, Oloko-Oba MI, Betiku E. Biodiesel production intensification via microwave irradiation-assisted transesterification of oil blend using nanoparticles from elephant-ear tree pod husk as a base heterogeneous catalyst. Chemical Engineering and Processing - Process Intensification. 2019 Jun;140:157–70. <DOI>.

23. Menkiti MC, Agu CM, Udeigwe TK. Extraction of oil from Terminalia catappa L.: Process parameter impacts, kinetics, and thermodynamics. Industrial Crops and Products. 2015 Dec;77:713–23. <DOI>.

24. Esonye C, Onukwuli OD, Ofoefule AU. Optimization of methyl ester production from Prunus Amygdalus seed oil using response surface methodology and Artificial Neural Networks. Renewable Energy. 2019 Jan;130:61–72. <DOI>.

25. Elkelawy M, Bastawissi HA-E, Esmaeil KK, Radwan AM, Panchal H, Sadasivuni KK, et al. Maximization of biodiesel production from sunflower and soybean oils and prediction of diesel engine performance and emission characteristics through response surface methodology. Fuel. 2020 Apr;266:117072. <DOI>.

26. Mäkelä M. Experimental design and response surface methodology in energy applications: A tutorial review. Energy Conversion and Management. 2017 Nov;151:630–40. <DOI>.

27. Abirami T, Loganaganandan M, Murali G, Fediuk R, Vickhram Sreekrishna R, Vignesh T, et al. Experimental research on impact response of novel steel fibrous concretes under falling mass impact. Construction and Building Materials. 2019 Oct;222:447–57. <DOI>.

28. Asfaram A, Ghaedi M, Ghezelbash GR, Pepe F. Application of experimental design and derivative spectrophotometry methods in optimization and analysis of biosorption of binary mixtures of basic dyes from aqueous solutions. Ecotoxicology and Environmental Safety. 2017 May;139:219–27. <DOI>.

29. Azari A, Noorisepehr M, Dehghanifard E, Karimyan K, Hashemi SY, Kalhori EM, et al. Experimental design, modeling and mechanism of cationic dyes biosorption on to magnetic chitosan-lutaraldehyde composite. International Journal of Biological Macromolecules. 2019 Jun;131:633–45. <DOI>.

30. Umanath K, Palanikumar K, Sankaradass V, Uma K. Optimization of wear properties on AA7075/Sic/Mos2 hybrid metal matrix composite by response surface methodology. Materials Today: Proceedings. 2021;46:4019–24. <DOI>.

31. Twisk J, Bosman L, Hoekstra T, Rijnhart J, Welten M, Heymans M. Different ways to estimate treatment effects in randomised controlled trials. Contemporary Clinical Trials Communications. 2018 Jun;10:80–5. <DOI>.

32. Sitepu EK, Heimann K, Raston CL, Zhang W. Critical evaluation of process parameters for direct biodiesel production from diverse feedstock. Renewable and Sustainable Energy Reviews. 2020 May;123:109762. <DOI>.

33. Al-Muhtaseb AH, Osman AI, Murphin Kumar PS, Jamil F, Al-Haj L, Al Nabhani A, et al. Circular economy approach of enhanced bifunctional catalytic system of CaO/CeO2 for biodiesel production from waste loquat seed oil with life cycle assessment study. Energy Conversion and Management. 2021 May;236:114040. <DOI>.

34. Klinger JL, Westover TL, Emerson RM, Williams CL, Hernandez S, Monson GD, et al. Effect of biomass type, heating rate, and sample size on microwave-enhanced fast pyrolysis product yields and qualities. Applied Energy. 2018 Oct;228:535–45. <DOI>.

35. Xiao R, Yang W, Cong X, Dong K, Xu J, Wang D, et al. Thermogravimetric analysis and reaction kinetics of lignocellulosic biomass pyrolysis. Energy. 2020 Jun;201:117537. <DOI>.

36. Lu H, Ip E, Scott J, Foster P, Vickers M, Baxter LL. Effects of particle shape and size on devolatilization of biomass particle. Fuel. 2010 May;89(5):1156–68. <DOI>.

37. Ambat I, Srivastava V, Sillanpää M. Recent advancement in biodiesel production methodologies using various feedstock: A review. Renewable and Sustainable Energy Reviews. 2018 Jul;90:356–69. <DOI>.

38. Hoseinzadeh Hesas R, Arami-Niya A, Wan Daud WMA, Sahu JN. Preparation of granular activated carbon from oil palm shell by microwave-induced chemical activation: Optimisation using surface response methodology. Chemical Engineering Research and Design. 2013 Dec;91(12):2447–56. <DOI>.

39. Peng WL, Mohd-Nasir H, Setapar SHM, Ahmad A, Lokhat D. Optimization of process variables using response surface methodology for tocopherol extraction from Roselle seed oil by supercritical carbon dioxide. Industrial Crops and Products. 2020 Jan;143:111886. <DOI>.

40. Yadav KK, Gupta N, Kumar V, Khan SA, Kumar A. A review of emerging adsorbents and current demand for defluoridation of water: Bright future in water sustainability. Environment International. 2018 Feb;111:80–108. <DOI>.

41. Bibi R, Ahmad M, Gulzar A, Tariq M. Effect of profenofos and citrus oil on Cryptolaemus montrouzieri Mulsant and Chrysoperla carnea Stephens, key predators of citrus mealybug, Planococcus citri (Risso), under laboratory conditions. Int J Trop Insect Sci. 2022 Feb;42(1):379–87. <DOI>.

42. Redondo D, Venturini ME, Luengo E, Raso J, Arias E. Pulsed electric fields as a green technology for the extraction of bioactive compounds from thinned peach by-products. Innovative Food Science & Emerging Technologies. 2018 Feb;45:335–43. <DOI>.

43. Chen Q, Dong W, Wei C, Hu R, Long Y. Combining integrated ultrasonic-microwave technique with ethanol to maximise extraction of green coffee oil from Arabica coffee beans. Industrial Crops and Products. 2020 Sep;151:112405. <DOI>.

44. Rehan M, Gardy J, Demirbas A, Rashid U, Budzianowski WM, Pant D, et al. Waste to biodiesel: A preliminary assessment for Saudi Arabia. Bioresource Technology. 2018 Feb;250:17–25. <DOI>.

45. Lacouture ME, Elizabeth Davis M, Elzinga G, Butowski N, Tran D, Villano JL, et al. Characterization and Management of Dermatologic Adverse Events With the NovoTTF-100A System, a Novel Anti-mitotic Electric Field Device for the Treatment of Recurrent Glioblastoma. Seminars in Oncology. 2014 Jun;41:S1–14. <DOI>.

46. Chhabra M, Dwivedi G, Baredar P, Kumar Shukla A, Garg A, Jain S. Production & optimization of biodiesel from rubber oil using BBD technique. Materials Today: Proceedings. 2021;38:69–73. <DOI>.